Pseudopapilledema Diagnosis based on a Hybrid Approach Using Deep Transfer Learning

Athar Al-azzawi
Electrical and Computer Engineering
Altinbaş University
Istanbul, Turkey
223720858@ogr.altinbas.edu.tr

Saif Al-jumaili
Electrical and Computer Engineering
Altinbaş University
Istanbul, Turkey
saifabdalrhman@gmail.com

Adil Deniz Duru
Sports And Health Sciences
Marmara University
Istanbul, Turkey
deniz.duru@marmara.edu.tr

Oguz Bayat
Electrical and Computer Engineering
Altinbas University
Istanbul, Turkey
oguz.bayat@altinbas.edu.tr

Sefer Kurnaz
Computer Engineering
Altinbas University
Istanbul, Turkey
sefer.kurnaz@altinbas.edu.tr

Osman Nuri Uçan
Electrical and Computer Engineering
Altinbas University
Istanbul, Turkey
osman.ucan@altinbas.edu.tr

2023 7th International Symposium on Multidisciplinary Studies and Innovative Technologies (ISMSIT) | 979-8-3503-4215-4/23/$31.00 ©2023 IEEE | DOI: 10.1109/ISMSIT58785.2023.10304843

***Abstract*—This Papilledema is edema caused by elevated pressure inside the brain near the area that leads the optic nerve to reach the eye. If left untreated, this condition can cause severe difficulties, for instance, aberrant optical changes, reduced sharpness of vision, and irreversible blindness. At present, an approach based on image processing for determining the degree of papilledema from color fundus images was given utilizing transfer learning approaches. The used dataset here contains 295 papilledema images, 295 pseudopapilledema images, and 779 control images. For the image preparation, a segmentation optimizer was utilized. The performance of the transfer learning techniques GoogleNet, MobileNetV2, ResNet-18, and ResNet-50 was then compared. Furthermore, Sensitivity and specificity and constructed ROC curves were calculated. The ResNet-50 employing the optimizer ADAM method performed best in the testing, with 98% total accuracy. The findings of the studies demonstrated that a combination of segmentation, optimization models, and transfer learning techniques may be utilized to determine the severity of papilledema automatically. The total accuracy was higher when compared to other similar studies described in the literature.**

Keywords— papilledema, pseudopapilledema, googlenet, mobilenetv2, resnet-18, resnet-50.

I. INTRODUCTION

This Pseudopapilledema (PPE) refers to an optic nerve abnormality characterized by elevation of the optic disc surface and blurring of its boundaries, due to the calcific entities located within the optic nerve head and also considered as a benign condition [1]. Meanwhile, it might mimic papilledema or disc edema seen in ocular neuropathies. On the other hand, Papilledema is a medical term that refers to actual swelling (edema) of the optic disc caused by high intracranial pressure (ICP). It can be produced by an intracranial lesion that takes up space, such as a tumor or hemorrhage. However, papilledema is frequently linked with an unexplained rise in ICP, a disease known as pseudotumor cerebri or benign intracranial hypertension. Symptoms frequently impact both eyes at the same time. A change in posture, such as rapidly rising up, causes visual blackouts. The most frequent symptom is headache. Other symptoms include momentary blindness, loss of vision owing to optical abnormalities, tinnitus, and nausea. People who are overweight or obese, obese, and obese women of reproductive age are at a slightly greater risk of papilledema [2]. Patients suffering from pseudopapilledema may experience major complications if the essential therapies are not used. It is a condition that can have an impact on a person's career, family life, education, and, most significantly, life.

In order to diagnose these diseases, it may be required a detailed examination of the disc morphology, due to the optic disc in papilledema and pseudopapilledema might seem identical on the outside. Noteworthy, PPE is a harmless illness, but it must be distinguished from other ocular neuropathies, where the exact diagnosis decreases unnecessary scans and offers the patient therapeutic options with minimum time. Multimodal imaging analysis, such as B-scan ultrasonography, fundus photography, autofluorescence, fluorescein angiography, and optical coherence tomography (OCT), has recently offered significant information for the precise diagnosis of PPE [3]. In ophthalmology, it can be hard to diagnose or detect a variety of diseases, such as diabetic eye disease, Stargardt disease, and glaucoma therefore deep learning plays a role part role in assisting the diagnosis process [4-7]. Deep learning is A technology belonging to artificial intelligence (AI) which its job trying to train computers to work like a human brain when dealing and analyzing data. Besides these datasets, there is computed tomography (CT) can be used, also there is the magnetic resonance imaging (MRI) instead of ultrasonography to acquire comprehensive cross-sectional pictures to discriminate disease [8-12]. In contrast to X-rays and CT scans, MRI does not expose patients to ionizing radiation (harmful ionizing radiation) [13]. However, because of the high cost of the instrument, high expenditures, and expensive contrast medication, it is an expensive testing approach [14]. We evaluated deep learning's accuracy and sensitivity for distinguishing between PPE, ocular neuropathies, and normal using subjects who haven't replaced their visual function and optic nerve head over a period of more than a year. This study included 177 cases of ischemic optic neuropathy, 48 cases of optic neuritis, 17 cases of diabetic optic neuropathy, 22 cases of papilledema, and 31 cases of retinal diseases such as central retinal vein occlusion or posterior uveitis in the optic neuropathies category.

II. LITERATURE REVIEW

In comparison to other neurological illnesses, there are less studies that use transfer learning algorithms to identify papilledema and pseudopapilledema. Gómez-Valverde et al. [15], used the VGG-19 architecture for glaucoma detection and got an AUC of 94%. In the identification of optic disc anomalies, Liu et al. [16], achieved an AUC of 99% using the ResNet-152 architecture. Milea et al. [17], distinguished optic

979-8-3503-4215-4/23/$31.00 ©2023 IEEE

disc anomalies from papilledema using the segmentation network U-Net architecture. Using DenseNet-121 and DenseNet-201 architectures for classification, they attained the maximum accuracy rate of 91.8%.

To detect the degree of papilledema, Vasseneix et al. [18], employed U-Net segmentation. They achieved 87.9% classification accuracy using the VGGNet architecture. Bakr and Ylmaz [19], employed VGG-16, ResNet, InceptionV3, and MobileNet architectures for cataract diagnosis, with ResNet achieving the greatest accuracy rate of 95.51%. Ahn et al. [7] used Gaussian filtering, picture normalization, and image cropping to detect ocular neuropathies and pseudopapilledema. VGG19, ResNet50, InceptionV3, and their own model were employed.

In the ResNet50 architecture, they attained the greatest accuracy of 98.63%. The development of image processing-based transfer learning models for the diagnosis of pseudopapilledema and papilledema is an issue that is still being investigated. The use of picture pre-processing and filtering procedures in transfer learning methodologies can result in high performance. A diagnostic system is required to simply and accurately diagnose these problems, Letter file.

III. Materials and Methods

A. Datasets

The datasets used here were provided by Kim's Eye Hospital, with a total count of 1369 images, subdivided as follows: 295 images of optic neuropathies, 295 of PPE, and 779 normal images, Fig. 1 is explored the datasets classes.

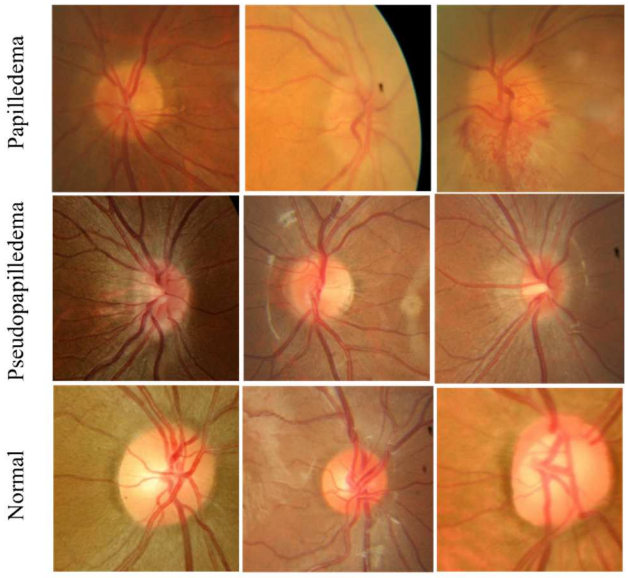

Fig. 1. The Dataset According to The Classes.

The datasets were resized to a set width of 500 pixels with a fixed ratio of the aspect. Moreover, to obtain the fixed-size input required by machine learning models, each image was clipped with a size of 240 x 240 pixels at the optic nerve area. Next, we segmented the images which is a critical job in medical image processing. Where Deep learning has made major advances in image segmentation. In addition, developing and training segmentation models for medical datasets is considered impossible owing to the costly and time-consuming nature of gathering and curating medical data, primarily because radiologists must be cautious in their interpretations.

B. Convolutional Neural Network

Four well-known pre-trained CNNs were employed in this work to discriminate between PPE and increased optic disc associated with optic neuropathies: GoogleNet, MobileNet-V2, ResNet-18, and ResNet-50 are the first three networks. As indicated in Fig. 2, the study was carried out in four stages: dataset analysis, data segmentation, optimization, and model evaluation. MATLAB software version R2021a was used for all data processing for model creation and validation.

GoogleNet is a deep model that has been trained using the ImageNet or Places365 datasets. The network consists of 22 layers, beginning with three convolution layers, followed by nine inception blocks, and eventually a fully connected layer [20]. MobileNet-V2 is a 53-layer deep CNN (52 convolution and one fully linked layer) [21]. The network's major portion design is built on inverted residual and linear bottlenecks. The network begins with three convolution layers, then moves on to 16 inverted residual and linear bottleneck blocks before concluding with one convolution layer and one fully connected layer.

ResNet is a deep network that is built on residual learning. By using the layer inputs as a reference, this type of learning can help with network training [22]. ResNet-18, ResNet-50, and ResNet-101 are all variants of ResNet that have their own residual block. ResNet-18 has 22 layers and starts with a convolution layer, then 8 residual blocks, and finally a fully connected layer. ResNet-50 is similar to ResNet-18, but it uses a different residual block structure and has a different number of residual blocks (16). ResNet-50 has 50 layers, while ResNet-101 has 50 layers as well. As a result, it has 101 layers and 33 leftover blocks.

C. Model Optimization

The DCNN model's performance was further investigated using optimizers. The optimizer was used to improve training accuracy while minimizing loss. The proposed research looked at the model's performance utilizing three optimizers: Adaptive Moment Estimation (ADAM), Root Mean Square Propagation (RMSProp), and Stochastic Gradient Descent with Momentum (SGDM). Furthermore, as demonstrated in Equation 1, the SGDM was used to accelerate gradient vectors on the appropriate route for quicker convergence.

$$\left.\begin{aligned} m_t &= \beta m_{t-1} + (1-\beta)\frac{\delta C}{\delta W} \\ W_t &= W_{t-1} - \alpha * m_t \end{aligned}\right\} \quad (1)$$

When μt and μt-1 denote momentum at t and t-1, respectively.

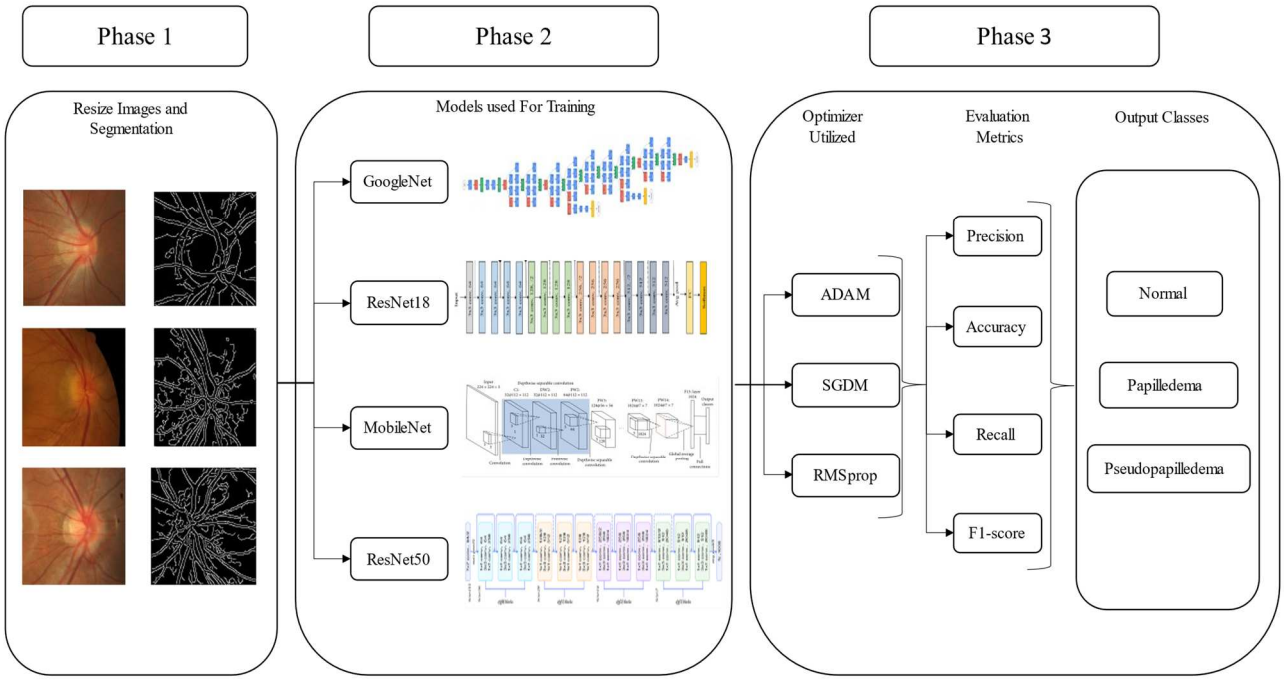

Fig. 2. The Suggested Transfer Learning Model Flow Diagram.

The RMSProp optimizer works by averaging to separate the learning rate for each weight, the magnitudes of recent gradients for the weights [23]. Equation 2 is an improved optimizer that computes this.

$$\left.\begin{aligned} R\left[g^2\right]_t &= \beta\, R\left[g^2\right]_{t-1} + (1-\beta)\left(\frac{\delta C}{\delta W}\right)^2 \\ W_t &= W_{t-1} - \frac{\alpha}{\sqrt{R[g^2]_t}} * \frac{\delta C}{\delta W} \end{aligned}\right\} \tag{2}$$

The ADAM optimizer relies on the merits of the previous two approaches to provide a more optimized gradient descent [24]. Equation 3 is an enhanced optimizer. For a negative sign, use a long dash rather than a hyphen.

$$\left.\begin{aligned} m_t &= \beta_1 m_{t-1} + (1-\beta_1)\frac{\delta C}{\delta W} \\ s_t &= \beta_2 s_{t-1} + (1-\beta_2)\left(\frac{\delta C}{\delta W}\right)^2 \\ \widehat{m_t} &= \frac{m_t}{1-\beta_1^t} \\ \widehat{s_t} &= \frac{s_t}{1-\beta_2^t} \\ W_t &= W_{t-1} - \frac{\alpha * \widehat{m_t}}{\sqrt{\widehat{s_t}+\varepsilon}} \end{aligned}\right\} \tag{3}$$

Where, β1, β2 are decay factors for gradient moments, ε is a tiny scalar used to prevent division by 0.

IV. Results And Discussions

Images of pseudopapilledema patients, papilledema patients, and control participants were included in the dataset utilised in this investigation. Kim's Eye Hospital pseudopapilledema data was used to generate colour fundus pictures [13]. There are 295 photos of pseudopapilledema, 295 photographs of papilledema, and 779 control images. Transfer learning algorithms were employed to assist in the automated detection of pseudopapilledema and papilledema. The photos were downsized in accordance with the transfer learning techniques' image input dimensions. "sgdm, adAm, and rmsprop" were the optimizers employed in this investigation. Figures 3,4, and 5 depict the confusion matrices for the four CNNs employed.

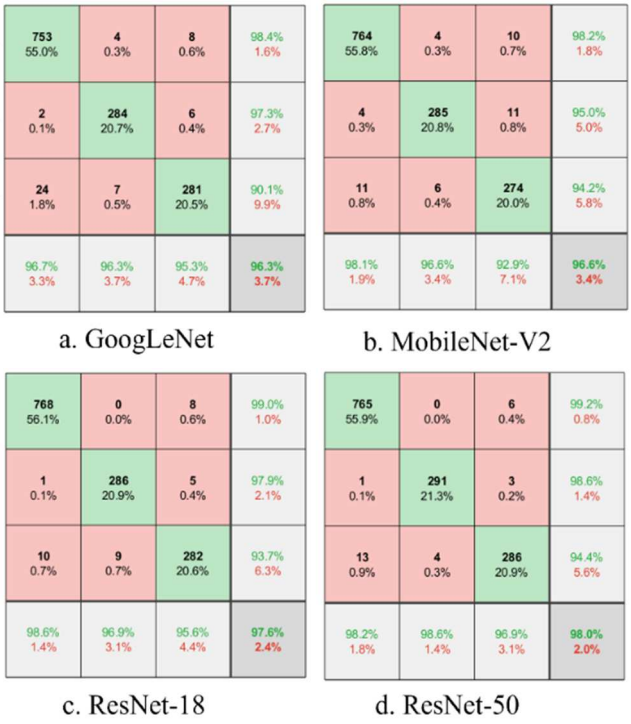

Fig. 3. Confusion matrices using ADAM Optimizer.

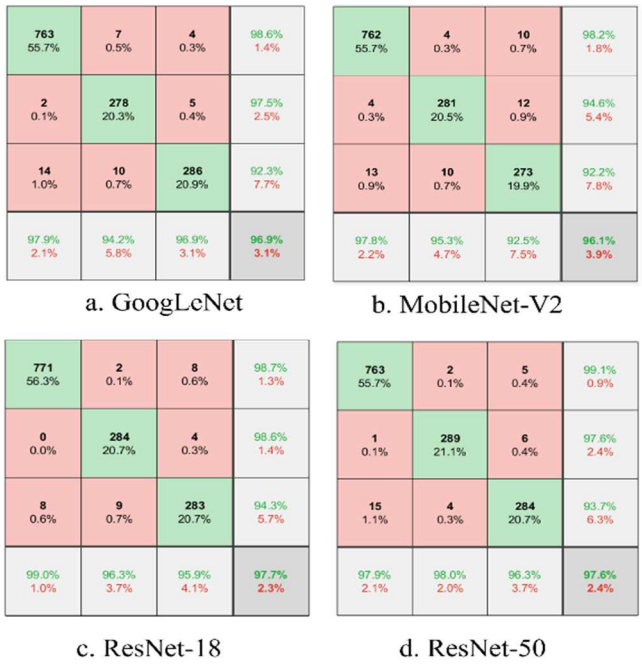

Fig. 4. Confusion matrices using RMSPROP Optimizer.

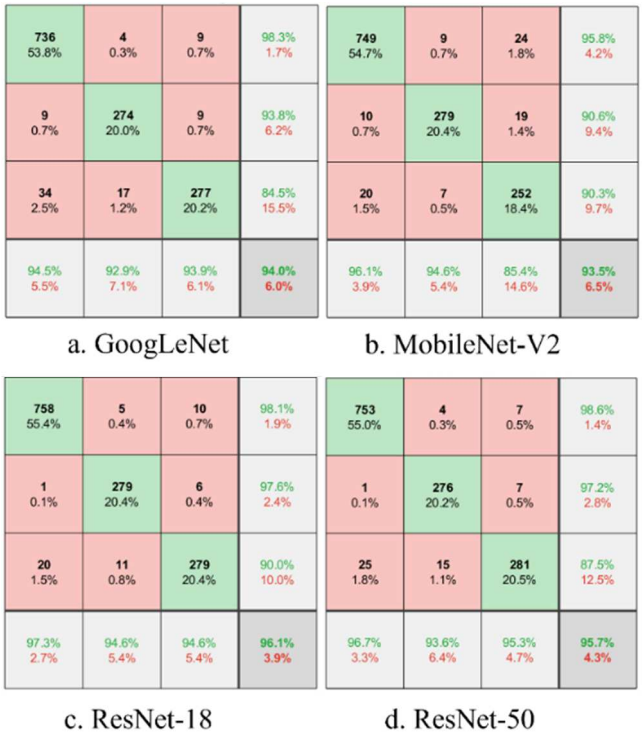

Fig. 5. Confusion matrices using SGDM Optimizer.

A. Evaluation Metrics

Different metric values may be discovered using the confusion matrix, and the model correctness can be examined in detail according to the method. The model takes an image and performs mathematical calculations described by training the model, yielding three probabilities. These probabilities represent the classes of the datasets are normal subjects, PPE, and papilledema. We also evaluated each model's micro-averaged sensitivity and specificity and constructed the ROC (receiver operating characteristic) curve, which shows how effectively the models categorize pictures into three categories (Normal, pseudopapilledema , and papilledema). According to Equation 4, accuracy is defined by the proportion of forecasts in the overall dataset that were correct. The total number of correct positive predictions from each positive prediction is used to calculate recall or sensitivity shown in Equation 5. Precision, also known as confidence, is the probability that an actual number will be larger than the total number of anticipated positives, as shown in Equation 6. While the balance of precision and memory is represented in Equation 7 by a harmonic, sometimes known as the F1-Score, the combination of precision and recall is represented. Using F1-Score is a secure technique to get a clear sense of the results we received.

$$Accuracy = \frac{TP + TN}{TP + FP + TN + FN} \tag{4}$$

$$Recall = \text{Sensitivity} = \frac{TP}{TP + FN} \tag{5}$$

$$Precision = Confidence = \frac{TP}{TP + Fp} \tag{6}$$

$$F1 - score = \frac{2 * TP}{2 * TP + FP + FN} \tag{7}$$

TABLE I. THE CLASSIFICATION PERFORMANCE RESULTS OF GOOGLENET MODEL.

	Optimizer	F1 Score	Precision	Recall	Acc%
GoogleNet	ADAM	98	98	97	96.2
		97	97	96	
		93	90	95	
	RMSPROP	97	98	96	96.9
		96	95	96	
		92	90	93	
	SGDM	96	98	94	94
		93	94	93	
		89	84	94	

TABLE II. THE CLASSIFICATION PERFORMANCE RESULTS OF MOBILENET-V2 MODEL.

	Optimizer	F1 Score	Precision	Recall	Acc%
MobileNet-V2	ADAM	98	98	98	96.6
		96	95	97	
		94	94	93	
	RMSPROP	98	98	98	96.1
		95	95	95	
		92	92	93	
	SGDM	96	96	96	93.4
		93	91	95	
		88	90	85	

TABLE III. THE CLASSIFICATION PERFORMANCE RESULTS OF RESNET-18 MODEL.

	Optimizer	F1 Score	Precision	Recall	Acc%
ResNet-18	ADAM	99	99	99	97.5
		97	98	97	
		95	94	96	
	RMSPROP	99	99	99	97.7
		97	99	96	
		95	94	96	
	SGDM	98	98	97	96.1
		96	98	95	
		92	90	95	

TABLE IV. THE CLASSIFICATION PERFORMANCE RESULTS OF RESNET-50 MODEL.

	Optimizer	F1 Score	Precision	Recall	Acc%
ResNet-50	ADAM	99	99	98	97.5
		99	99	99	
		96	94	97	
	RMSPROP	99	99	98	97.5
		98	98	98	
		95	94	96	
	SGDM	98	99	97	95.6
		95	97	94	
		91	88	95	

All of the experiments have been validated using the four performance measures described above. The influence of various characteristics on CNN models is tested in the first experiment, and the findings for the GoogleNet model are given in Table 1. Table 2 demonstrates the performance when the CNN model is changed, and it is clear that the best outcome for MobileNet-V2 was with ADAM. Tables 3 and 4 further shows that the ResNet-18 and ResNet-50 model performs. Furthermore, we constructed the ROC (receiver operating characteristic) curve, which shows how effectively the models categorize pictures into three categories (Normal, pseudopapilledema , and papilledema). Table 5 shows the accuracy of the transfer learning research in the literature and the proposed model. Vasseneix et al obtained 87.9% accuracy utilising the VGGNet architecture in comparable tests using the data sets utilized in the study [18]. Using the ResNet architecture, Bakr et al obtained 95.51% accuracy [19]. On the MobileNetV2 architecture, the suggested model obtained 96.83% accuracy by employing methodologies and designs that differed from the picture preprocessing/segmentation methods and transfer learning structures utilized in other models in the literature.

TABLE V. COMPARISON OF THE ACCURACY (ACC) VALUES AS A RESULT OF OUR PROPOSED METHOD WITH OTHER PAPERS.

Ref.	Image Prep. / Segm.	Datasets	No. of Classes	No. of Images		CNN	ACC%
				Total	Per-class		
2019 [15]	RZ-images	RIM-ONE [25],DRISHTI-GS [26], and Private	2	2,313	494 Glaucoma	VGG-19	94
					1819 NR		
2021 [18]	NON	Private	2	2,103	1052 Mild-Moderate Pap.	VGGNet	87
					1051 Severe Pap.		
2022 [19]	RZ-images Pixel Norm.	Private	2	1,094	304 Lf. Cat.	ResNet	95
					290 Rt. Cat.		
					250 Lf. NR		
					250 Rt. NR		
2023 [27]	RZ-images Hstg. 3-D box filtering.	Kim's Eye Hospital	3	1,369	295 Pap.	MobileNetV2	96
					295 pseud.		
					779 NR		
Proposed	**R-images Segm. Optimiz.**	**Kim's Eye Hospital**	**3**	**1,369**	**295 Pap.**	**ResNet-50**	**98**
					295 pseud.		
					779 NR		

V. CONCLUSION

In this work, a technique for classifying pseudopapilledema and papilledema using datasets with three separate classifications is provided. In the proposed method, the dataset images are resized and image pre-processing methods such as image segmentation and optimization model are applied. In transfer learning methodologies, the performances of pre-processed pictures are compared. As transfer learning methodologies, the GoogleNet, MobileNetV2, ResNet-18, and ResNet-50 architectures were employed. Performance evaluation metrics, namely accuracy, recall, F1-score, precision, specificity, and overall accuracy, were evaluated. It was discovered in the study that picture pre-processing methods and transfer learning approaches performed well. ResNet-50 with ADAM optimization model architecture was the best-performing transfer learning strategy, with 0.98 total accuracy. The proposed approach can assist professionals with their hectic work schedules as well as the early diagnosis of pseudopapilledema and papilledema. The experimental findings demonstrate that the proposed model can reach the high performance obtained by employing the picture preprocessing methods and transfer learning approaches utilized in earlier research using different methods and transfer learning approaches. This research will aid in the identification of pseudopapilledema and papilledema automatically.

REFERENCES

[1] G. L. Trick, S. S. Bhatt, D. Dahl, and B. Skarf, "Optic disc topography in pseudopapilledema: a comparison to pseudotumor cerebri," *Journal of neuro-ophthalmology,* vol. 21, no. 4, pp. 240-244, 2001.

[2] E. İbrahimov, "Optik disk kabarıklığında retina sinir lifi tabakası kalınlığının OCT ve HRT ile değerlendirilmesi," Dokuz Eylül Üniversitesi Tıp Fakültesi, 2009.

[3] M. A. Fard, S. Okhravi, S. Moghimi, and P. S. Subramanian, "Optic nerve head and macular optical coherence tomography measurements in papilledema compared with pseudopapilledema," *Journal of Neuro-Ophthalmology,* vol. 39, no. 1, pp. 28-34, 2019.

[4] V. Gulshan *et al.*, "Development and validation of a deep learning algorithm for detection of diabetic retinopathy in retinal fundus photographs," *jama,* vol. 316, no. 22, pp. 2402-2410, 2016.

[5] S. J. Kim, K. J. Cho, and S. Oh, "Development of machine learning models for diagnosis of glaucoma," *PloS one,* vol. 12, no. 5, p. e0177726, 2017.

[6] E. Rahimy, "Deep learning applications in ophthalmology," *Current opinion in ophthalmology,* vol. 29, no. 3, pp. 254-260, 2018.

[7] J. M. Ahn, S. Kim, K.-S. Ahn, S.-H. Cho, K. B. Lee, and U. S. Kim, "A deep learning model for the detection of both advanced and early glaucoma using fundus photography," *PloS one,* vol. 13, no. 11, p. e0207982, 2018.

[8] A. Al-azzawi, S. Al-jumaili, A. D. Duru, D. G. Duru, and O. N. Uçan, "Evaluation of Deep Transfer Learning Methodologies on the COVID-19 Radiographic Chest Images," *Traitement du Signal,* vol. 40, no. 2, 2023.

[9] S. Al-Jumaili, A. Al-Azzawi, A. D. Duru, and A. A. Ibrahim, "Covid-19 X-ray image classification using SVM based on

Local Binary Pattern," in *2021 5th International Symposium on Multidisciplinary Studies and Innovative Technologies (ISMSIT)*, 2021, pp. 383-387: IEEE.

[10] S. Al-Jumaili, A. Al-Azzawi, O. N. Uçan, and A. D. Duru, "Classification of the Level of Alzheimer's Disease Using Anatomical Magnetic Resonance Images Based on a Novel Deep Learning Structure," in *Diagnosis of Neurological Disorders Based on Deep Learning Techniques*: CRC Press, 2023, pp. 29-46.

[11] R. Ali, S. Al-Jumaili, A. D. Duru, O. N. Uçan, A. Boyaci, and D. G. Duru, "Classification of brain tumors using MRI images based on convolutional neural network and supervised machine learning algorithms," in *2022 International Symposium on Multidisciplinary Studies and Innovative Technologies (ISMSIT)*, 2022, pp. 822-827: IEEE.

[12] A.-J. Saif, "Classification of COVID-19 Omicron variant using Hybrid Deep Transfer Learning based on X-Ray images chest," *Aurum Journal of Health Sciences,* vol. 4, no. 3, pp. 153-165.

[13] O. Orhan, "Magnetik Rezonans Görüntüleme Mrg Nin Klinik Uygulamaları Ve Endikasyonları," *Harran Üniversitesi Tıp Fakültesi Dergisi,* vol. 5, no. 2, pp. 31-40, 2008.

[14] B. Sarioğlu, "Türkiyede MR ve BT görüntüleme işlemlerinin Sosyal Güvenlik Kurumuna ekonomik yükünün değerlendirilmesi," Sosyal Bilimler Enstitüsü.

[15] J. J. Gómez-Valverde *et al.*, "Automatic glaucoma classification using color fundus images based on convolutional neural networks and transfer learning," *Biomedical optics express,* vol. 10, no. 2, pp. 892-913, 2019.

[16] T. A. Liu *et al.*, "Detection of optic disc abnormalities in color fundus photographs using deep learning," *Journal of Neuro-Ophthalmology,* vol. 41, no. 3, pp. 368-374, 2021.

[17] D. Milea *et al.*, "Artificial intelligence to detect papilledema from ocular fundus photographs," *New England Journal of Medicine,* vol. 382, no. 18, pp. 1687-1695, 2020.

[18] C. Vasseneix *et al.*, "Accuracy of a deep learning system for classification of papilledema severity on ocular fundus photographs," *Neurology,* vol. 97, no. 4, pp. e369-e377, 2021.

[19] H. BAKIR and Ş. YILMAZ, "Using Transfer Learning Technique as a Feature Extraction Phase for Diagnosis of Cataract Disease in the Eye," *International Journal of Sivas University of Science and Technology,* vol. 1, no. 1, pp. 17-33, 2022.

[20] C. Szegedy *et al.*, "Going deeper with convolutions," in *Proceedings of the IEEE conference on computer vision and pattern recognition*, 2015, pp. 1-9.

[21] M. Sandler, A. Howard, M. Zhu, A. Zhmoginov, and L.-C. Chen, "Mobilenetv2: Inverted residuals and linear bottlenecks," in *Proceedings of the IEEE conference on computer vision and pattern recognition*, 2018, pp. 4510-4520.

[22] K. He, X. Zhang, S. Ren, and J. Sun, "Deep residual learning for image recognition," in *Proceedings of the IEEE conference on computer vision and pattern recognition*, 2016, pp. 770-778.

[23] N. Qian, "On the momentum term in gradient descent learning algorithms," *Neural networks,* vol. 12, no. 1, pp. 145-151, 1999.

[24] D. P. Kingma and J. Ba, "Adam: A method for stochastic optimization," *arXiv preprint arXiv:1412.6980,* 2014.

[25] F. Fumero, S. Alayón, J. L. Sanchez, J. Sigut, and M. Gonzalez-Hernandez, "RIM-ONE: An open retinal image database for optic nerve evaluation," in *2011 24th international symposium on computer-based medical systems (CBMS)*, 2011, pp. 1-6: IEEE.

[26] J. Sivaswamy, S. Krishnadas, G. D. Joshi, M. Jain, and A. U. S. Tabish, "Drishti-gs: Retinal image dataset for optic nerve head (onh) segmentation," in *2014 IEEE 11th international symposium on biomedical imaging (ISBI)*, 2014, pp. 53-56: IEEE.

[27] M. Kokulu and H. Göker, "Detection of Papilledema Severity from Color Fundus Images using Transfer Learning Approaches," *Aksaray University Journal of Science and Engineering,* vol. 7, no. 2, pp. 53-61, 2023.